Excitonic Effects on the Optical Response of Graphene and Bilayer Graphene

Li Yang, Jack Deslippe, Cheol-Hwan Park, Marvin L. Cohen, and Steven G. Louie

Department of Physics, University of California at Berkeley, Berkeley, California 94720, USA and Materials Sciences Division, Lawrence Berkeley National Laboratory, Berkeley, California 94720, USA

(Received 2 June 2009; published 28 October 2009)

We present first-principles calculations of many-electron effects on the optical response of graphene, bilayer graphene, and graphite employing the *GW*-Bethe Salpeter equation approach. We find that resonant excitons are formed in these two-dimensional semimetals. The resonant excitons give rise to a prominent peak in the absorption spectrum near 4.5 eV with a different line shape and significantly redshifted peak position from those of an absorption peak arising from interband transitions in an independent quasiparticle picture. In the infrared regime, our calculated optical absorbance per graphene layer is approximately a constant, 2.4%, in agreement with recent experiments; additional low frequency features are found for bilayer graphene because of band structure effects.

DOI: 10.1103/PhysRevLett.103.186802 PACS numbers: 73.22.−f, 72.80.Rj, 75.70.Ak

Excitonic effects are observable in the optical response of semiconductors. Earlier work based on a tight-binding bond-orbital model illustrated these effects in bulk semiconductors [1] and *ab initio* methods employing the *GW*-Bethe-Salpeter equation (*GW*-BSE) approach have become available in the past decade [2]. Excitonic effects are commonly believed to be unimportant in the optical spectrum of metals because of strong screening. However, recent first-principles calculations [3,4] have predicted, and subsequent experimental studies [5] have confirmed, the existence of bound excitons in one-dimensional (1D) metallic carbon nanotubes (CNTs). Therefore, it is of considerable interest to explore whether there are significant excitonic effects in 2D metallic or semimetallic systems.

Graphene is a 2D semimetal with interesting physics associated with its unusual electronic structure and its promising device applications [6–8]. In particular, the optical properties of graphene display many intriguing features, such as a constant optical conductivity in the infrared regime and gate-dependent optical absorbance [9–12]. However, there have been no first-principles studies to date of optical properties of graphene including excitonic effects that are known to be important in reduced dimensional materials.

In this work, we have carried out first-principles calculations using a many-body Green's function theory to study the optical spectra of graphene and bilayer graphene. Following the approach of Rohlfing and Louie [13], we calculate the optical response of isolated single- and bilayer intrinsic graphene in three stages: (i) we obtain the electronic ground state using density functional theory (DFT) within the local density approximation (LDA); (ii) the quasiparticle excitations are calculated within the *GW* approximation [14]; and (iii) we solve the Bethe-Salpeter equation (BSE) to obtain the photo-excited states and optical absorption spectra [1,2,13].

Our first-principles results on graphene show that, for single-particle excitations, there is a significant self-energy correction to the band velocity of the Dirac quasiparticles. Owing to electron-hole interaction, the absorption peak arising from the interband transitions at around 5.1 eV is totally suppressed and replaced by a new peak at 4.5 eV with a very different line shape. This change in the optical spectrum is the result of a redistribution of optical transition strengths by strong resonant excitons. These results persist in bilayer graphene. Moreover, the calculated infrared spectral absorbance per graphene layer including electron-hole interactions is approximately a constant, 2.4%, in agreement with recent experiments [10,11].

In our studies, the intralayer structure of graphene and bilayer graphene is fully relaxed within DFT/LDA. For Bernal-stacked bilayer graphene, the interlayer distance is chosen to be the experimental value of graphite (0.334 nm). The calculations are done in a supercell arrangement [15] with a plane-wave basis using norm-conserving pseudopotentials [16] with a 60 Ry energy cutoff. The distance between graphene sheets in neighboring supercells is 1.2 nm to avoid spurious interaction. A $32 \times 32 \times 1$ k-point grid is used to ensure converged LDA results and a $64 \times 64 \times 1$ k-point grid is necessary for computing the converged self-energy. We take into account dynamical screening effects in the self-energy through the generalized plasmon pole model [14]. In solving the BSE, we make two approximations: (i) the Tamm-Dancoff approximation, which has given accurate results for the optical absorption spectra of other metallic systems such as metallic CNTs [3,4], and (ii) the static electron-hole interaction approximation since the excitation energy of excitons is large ($\sim$5 eV) relative to the electron-hole interaction energy. The electron-hole interaction kernel is evaluated first on a coarse k grid ($64 \times 64 \times 1$) and then interpolated onto a fine grid ($200 \times 200 \times 1$) [13]. Two valence bands and two conduction bands are included for calculating the optical absorption spectra and inclusion of more bands does change the spectra in the 0–7 eV range. In the discussion below, we shall focus on the absorption spectra for light polarized parallel to the graphene plane with a Lorentzian broadening of 0.05 eV.

The LDA Kohn-Sham eigenvalues and *GW* quasiparticle band structure of graphene close to the Dirac point are shown in Fig. 1(a). While the LDA Fermi velocity of graphene is 0.85×10^6 m/s, the *GW* value is 1.15×10^6 m/s that is in good agreement with experiment [7] as well as with previous *GW* calculations [17,18]. The LDA and quasiparticle band structures of bilayer graphene close to the Dirac point are shown in Fig. 1(b).

Figure 2(a) shows the calculated optical spectrum of graphene. The plotted quantity $\alpha_2(\omega)$ is the imaginary part of the polarizability per unit area and is obtained by multiplying the calculated dielectric susceptibility, $\chi = (\varepsilon - 1)/4\pi$, by the distance between adjacent graphene layers (or bilayers) in our supercell arrangement. This quantity $\alpha_2(\omega)$ when multiplied by the area of graphene or bilayer graphene gives the polarizability. The absorption below 0.3 eV is not shown because intraband transitions and temperature effects are important there and our calculation does not include these factors. In absence of electron-hole interactions, the interband transitions form a prominent absorption peak at 5.15 eV. However, with excitonic effects included, a prominent absorption peak now appears at 4.55 eV which is a 600 meV apparent shift. In addition, the peak profile is substantially modified from an almost symmetric peak to an asymmetric one in the excitonic case.

It is surprising to find such large excitonic effects (an apparent shift of 600 meV and a dramatic change in shape of the optical peak) in this 2D semimetal, given that the binding energy of excitons found in 1D metallic CNTs is only tens of meV and that there is no significant excitonic effect in bulk metals. In Fig. 2(b), we see that both the joint density states (JDOS) of quasiparticles from the *GW* calculation and the density of excitonic states from solving the BSE are nearly identical, similar to findings in bulk semiconductors [13]. These changes arise mainly from the attractive direct term of the electron-hole interaction kernel, with the repulsive exchange term plays a negligible role.

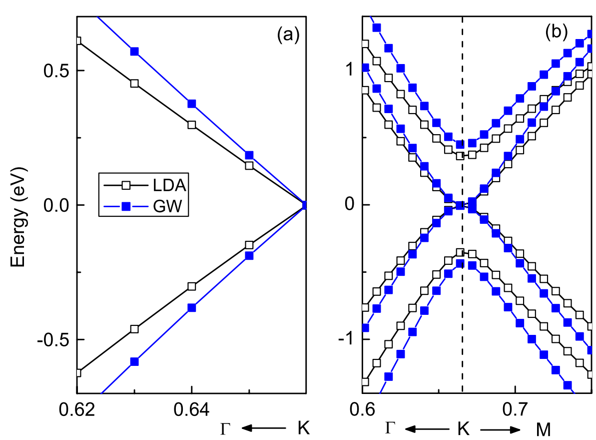

FIG. 1 (color online). LDA eigenvalues and *GW* quasiparticle energies of graphene (a) and bilayer graphene (b) close to the Dirac point. Wave vector is in $\frac{2\pi}{a}$, where a is the in-plane lattice constant.

To analyze our results, we rewrite the relevant optical transition matrix element for going from the ground state $|0\rangle$ to a correlated electron-hole (exciton) state $|i\rangle = \sum_k \sum_v^{\text{hole}} \sum_c^{\text{elec}} A_{vck}^i |vck\rangle$ into the form [13]

$$\langle 0|\vec{v}|i\rangle = \sum_v \sum_c \sum_k A_{vck}^i \langle vk|\vec{v}|ck\rangle = \int S_i(\omega) d\omega, \quad (1)$$

where

$$S_i(\omega) = \sum_{v,c,k} A_{vck}^i \langle vk|\vec{v}|ck\rangle \delta[\omega - (E_{ck} - E_{vk})], \quad (2)$$

which gives a measure of the contribution of all interband pairs (ck, vk) at a given transition energy ω to the optical strength of the exciton state i. Because of inversion symmetry of graphene, $S_i(\omega)$ is given as a real function. In Fig. 3, $S_i(\omega)$ and its integrated value up to a given frequency are depicted for three optically bright excited state to provide an understanding of why excitonic effects enhance the absorption around 4.5 eV but depress it around 5.1 eV.

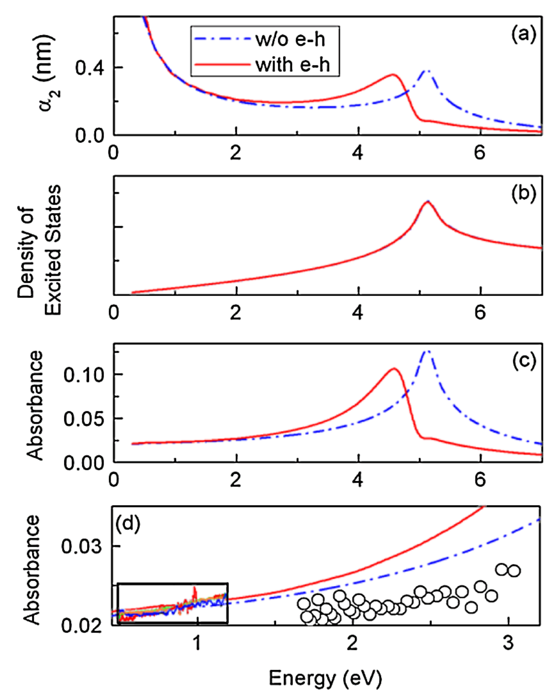

FIG. 2 (color online). (a) Optical absorption spectra, (b) density of excited states, (c) absorbance of graphene with and without excitonic effects included; and (d) comparison with experiments. In (d), rough colored curves within the small rectangular box are measurements from Ref. [11], and open circles are from those from Ref. [10].

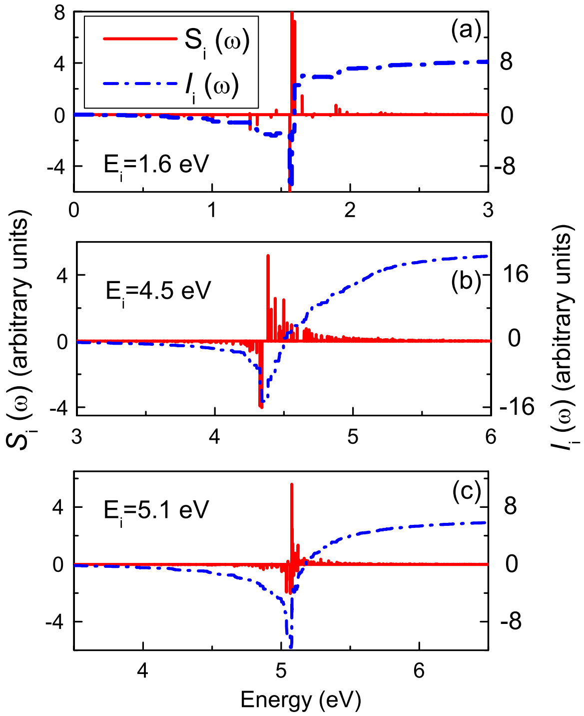

FIG. 3 (color online). $S_i(\omega)$ and the corresponding integration $I(\omega) = \int_0^\omega S_i(\omega')d\omega'$ of three optically bright states in graphene from GW-BSE calculations.

Figure 3(a) shows $S_i(\omega)$ for a state at 1.6 eV. Since there is negligible excitonic effect below 2.0 eV, this state displays a narrow energy distribution in $S_i(\omega)$. In Figs. 3(b) and 3(c), the states studied, located around 4.5 and 5.1 eV, respectively, show a considerably wider energy distribution in $S_i(\omega)$, indicating that they are linear combinations of many free electron-hole pair configurations of different energies which is consistent with having significant excitonic effects in this energy regime [19]. (The real-space wave functions of two resonant states are given in Ref. [20].)

In Fig. 3(b), the optical interband transition matrix element distribution for the state has larger amplitude extending to the high-energy direction. Since the running integrated value of $S_i(\omega)$ in Fig. 3(b) increases significantly from 4.5 to 5.5 eV which is exactly the range of the strong interband absorption peak, this particular resonant exciton steals optical transition strength from the prominent interband absorption peak around 5.1 eV and enhances the optical absorption around 4.5 eV. In contrast, the $S_i(\omega)$ for the state shown in Fig. 3(c) is more antisymmetric than that shown in (b). The negative and positive contributions above and below 5.1 eV, respectively, nearly cancel each other and the final integrated strength is only one-third of that of the exciton in (b). As a result, the optical absorption around 5.1 eV is depressed.

The infrared absorbance of graphene is expected to be a constant (2.29%) [9–11,21–27]. Figure 2(c) shows the calculated absorbance, $A(\omega) = \frac{4\pi\omega}{c}\alpha_2(\omega)$, of graphene with and without excitonic effects included. The infrared absorbance is nearly the same (around 2.4%) in both cases. Our result is in good agreement with measured values and is consistent with previous studies [28]. Figure 2(d) compares the calculated results to experimental data [10,11]. The calculated absorbance has a small but finite slope, in good agreement with measurements in Ref. [11]. The very small excitonic influence in the infrared regime may be attributed to a vanishing JDOS near zero energy.

The absorbance of bilayer graphene is presented in Fig. 4(a), showing similar excitonic effects as those in single-layer graphene, with a significant redshift of the prominent absorption peak around 5 eV. There is also a noticeable absorption feature at 0.4 eV, contributed by interband transitions near the Dirac point. Moreover, in Fig. 4(a), the infrared spectral absorbance is around 4.8%, twice that of graphene. The large excitonic effects in bilayer graphene near 4.5 eV have similar origins as those in graphene. However, as shown in Fig. 1(b), the lowest conduction band and the highest valence band in the bilayer case touch each other and have parabolic shape. This provides a larger DOS around the Fermi level and results in stronger screening than that of graphene. Therefore, as shown in Fig. 4(a), an apparent 450 meV redshift of the prominent absorption peak of bilayer graphene is obtained with excitonic effects, which is smaller than that of graphene (600 meV).

We give also the calculated optical absorption of graphite together with experimental results [29] in Fig. 4(b) and summarize the main absorption peak position of graphene, bilayer graphene, graphite and experimental data in Table I. Our results for graphite are in good accord with experiment. We note that self-energy corrections and excitonic effects nearly cancel each other, making the positions of the main absorption peak of all three structures

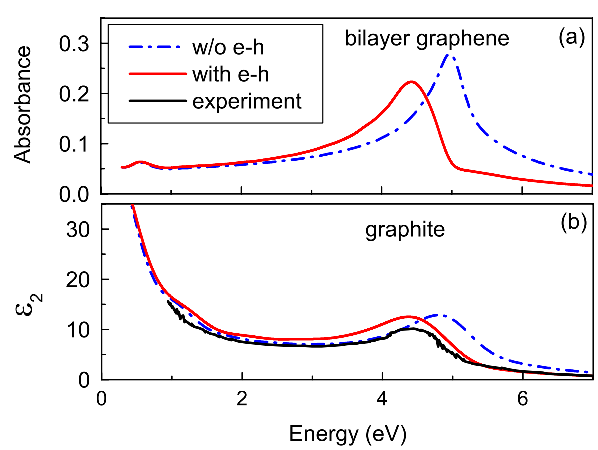

FIG. 4 (color online). (a) Absorbance of bilayer graphene and (b) imaginary part of the dielectric function of graphite with and without excitonic effects included. Experiment data of graphite [29] are included in (b).

TABLE I. Main absorption peak position (in eV) of graphene, bilayer graphene and graphite, and change in peak position rising from self-energy effects ($\delta\Sigma$) and from excitonic effects ($\delta_{\rm exciton}$).

	Graphene	Bilayer Graphene	Graphite
$E_{\rm peak}$ (Expt.)			4.55 [29]
$E_{\rm peak}$ (GW + BSE)	4.55	4.52	4.50
$\delta\Sigma$	+1.10	+0.91	+0.69
$\delta_{\rm exciton}$	−0.60	−0.45	−0.27

similar although the character of the excited states can change significantly. This near cancellation effect in excitation energies was noticed in other nanostructures previously [3,30,31].

In conclusion, we have performed first-principles calculations on the quasiparticle energies and optical properties of single- and bilayer graphene and graphite with many-electron effects included. Resonant excitonic effects in graphene and bilayer graphene result in significant changes in the optical absorption spectrum in the energy regime near a van Hove singularity as compared to the independent-particle picture. Finally, we have shown that excitonic effects do not change the absorbance in the infrared range from that calculated within the single-particle picture, in agreement with experimental findings.

We thank Y.-W. Son, D. Prendergast, and E. Kioupakis for discussions. L. Y. and J. D. and simulations studies were supported by the Director, Office of Science, Office of Basic Energy under Contract No. DE-AC02-05CH11231, and C.-H. P. and theoretical methods and codes were supported by NSF Grant No. DMR07-05941. J. D. received a DOE Computational Science Graduate Grant No. DE-FG02-97ER25308. Computational resources provided by Lonestar of teragrid at the Texas Advanced Computing Center.

[1] W. Hanke and L. J. Sham, Phys. Rev. B **21**, 4656 (1980); M. del Castillo-Mussot and L. J. Sham, Phys. Rev. B **31**, 2092 (1985).
[2] M. Rohlfing and S. G. Louie, Phys. Rev. Lett. **80**, 3320 (1998); Phys. Rev. Lett. **81**, 2312 (1998); S. Albrecht, L. Reining, R. Del Sole, and G. Onida, Phys. Rev. Lett. **80**, 4510 (1998); L. X. Benedict and E. L. Shirley, Phys. Rev. Lett. **80**, 4514 (1998).
[3] C. D. Spataru, S. Ismail-Beigi, L. X. Benedict, and Steven G. Louie, Phys. Rev. Lett. **92**, 077402 (2004).
[4] J. Deslippe, C. D. Spataru, D. Prendergast, and S. G. Louie, Nano Lett. **7**, 1626 (2007).
[5] Feng Wang *et al.*, Phys. Rev. Lett. **99**, 227401 (2007).
[6] K. S. Novoselov *et al.*, Science **306**, 666 (2004).
[7] Y. Zhang, Y.-W. Tan, H. L. Stormer, and P. Kim, Nature (London) **438**, 201 (2005).
[8] A. K. Geim and K. S. Novoselov, Nature Mater. **6**, 183 (2007); A. H. Castro Neto *et al.*, Rev. Mod. Phys. **81**, 109 (2009), and references therein.
[9] V. P. Gusynin and S. G. Sharapov, Phys. Rev. B **73**, 245411 (2006).
[10] R. R. Nair *et al.*, Science **320**, 1308 (2008).
[11] K. F. Mak *et al.*, Phys. Rev. Lett. **101**, 196405 (2008).
[12] F. Wang *et al.*, Science **320**, 206 (2008).
[13] M. Rohlfing and S. G. Louie, Phys. Rev. B **62**, 4927 (2000).
[14] M. S. Hybertsen and S. G. Louie, Phys. Rev. B **34**, 5390 (1986).
[15] M. L. Cohen, M. Schltüer, J. R. Chelikowsky, and S. G. Louie, Phys. Rev. B **12**, 5575 (1975).
[16] N. Troullier and J. L. Martins, Phys. Rev. B **43**, 1993 (1991).
[17] P. E. Trevisanutto *et al.*, Phys. Rev. Lett. **101**, 226405 (2008).
[18] C. Attaccalite, A. Greneis, T. Pichler, and A. Rubio, arXiv:0808.0786v2.
[19] The function $S_i(\omega)$ plotted changes sign as $\omega(k) = E_{ck} - E_{vk}$ crosses the excitation energy of the ith state. This "resonantlike" behavior is a consequence of the structure of the BSE which gives rise to a change in sign in the coefficient A as the interband transition energy of the contributing e-h pair configuration crosses the excitation energy. A similar sign change in the amplitude occurs in quantum mechanical scattering problems [e.g., J. J. Sakurai, *Modern Quantum Mechanics* (Addison-Wesley, Reading, MA, 1993), 2nd ed.].
[20] See EPAPS Document No. E-PRLTAO-103-007947 for supplementary information. For more information on EPAPS, see http://www.aip.org/pubservs/epaps.html.
[21] E. J. Nicol and J. P. Carbotte, Phys. Rev. B **77**, 155409 (2008).
[22] J. M. Dawlaty *et al.*, arXiv:cond-mat/08013302.
[23] T. Stauber, N. M. R. Peres, and A. K. Geim, Phys. Rev. B **78**, 085432 (2008).
[24] T. Ando, Y. S. Zheng, and H. Suzuura, J. Phys. Soc. Jpn. **71**, 1318 (2002).
[25] C. Zhang, L. Chen, and Z. Ma, Phys. Rev. B **77**, 241402 (2008).
[26] Z. Q. Li *et al.*, Phys. Rev. Lett. **102**, 037403 (2009).
[27] N. M. R. Peres, F. Guinea, and A. H. Castro Neto, Phys. Rev. B **73**, 125411 (2006).
[28] M. I. Katsnelson, Europhys. Lett. **84**, 37 001 (2008).
[29] E. A. Taft and H. R. Philipp, Phys. Rev. **138**, A197 (1965); A. B. Djurisic and E. H. Li, J. Appl. Phys. **85**, 7404 (1999).
[30] L. Yang, M. L. Cohen, and S. G. Louie, Nano Lett. **7**, 3112 (2007); D. Prezzi *et al.*, Phys. Rev. B **77**, 041404(R) (2008).
[31] L. Yang, C. D. Spataru, S. G. Louie, and M. Y. Chou, Phys. Rev. B **75**, 201304(R) (2007).